



Green synthesized silver and zinc oxide nanoparticles using *Ficus carica* leaf extract and their activity on human viruses

Ahmed A. Hmed¹, Atef S. El-Gebaly¹, Ehab E. Refaey¹, Ahmed R. Sofy¹ and Ahmed M. Youssef^{2*}

¹ Botany and Microbiology Department, Faculty of Science, Al-Azhar University, 11884 Nasr City, Cairo, Egypt

² Packaging materials Department, National Research Centre, 33 El Bohouth St. (former El Tahrir St.), Dokki, Giza, P.O. 12622, Egypt

In Loving Memory of Late Professor Doctor "Mohamed Refaat Hussein Mahran"

Abstract

The present study focuses on the eco-friendly synthesis of silver (Ag-NP) and zinc oxide (ZnO-NP) nanoparticles using *Ficus carica* leaf extract as a highly efficient reducing agent. The successful formation of (Ag-NP) and (ZnO-NP) was visually confirmed by observing the change in color or turbidity of the solutions. Additionally, characterization techniques such as UV-Vis spectroscopy, TEM, FT-IR, and XRD were employed to further investigate the synthesized nanoparticles. The UV-Vis spectrum exhibited a peak at 445, 380 nm, indicating the existence of Ag-NP and ZnO-NP, respectively. FT-IR analysis confirmed the presence of various functional groups and their corresponding bonds in the fabricated nanoparticles. Moreover, TEM analysis accurately determined the size in nanoform. The antiviral and cytotoxic activities of Ag-NP and ZnO-NP were evaluated against the H1N1 influenza virus, adenovirus, and Herpes Simplex Virus type 2 (HSV-2). Both types of nanoparticles showed antiviral properties against all viruses. For Adenovirus, ZnO-NP showed a CC₅₀ of 119.430 µg/ml, while Ag-NP showed a CC₅₀ of 190.18 µg/ml, indicating that ZnO-NP was relatively more cytotoxic. Ag-NP had a lower IC₅₀ of 22.585 µg/ml against HSV-2 when compared to ZnO-NP, which showed an IC₅₀ of (77.745 µg/ml), demonstrating the greater efficacy of Ag nanoparticles. For H1N1, Ag-NP had a lower IC₅₀ (23.03 µg/ml) than Zn nanoparticles (33.2 µg/ml), which displayed comparable outcomes. ZnO-NP showed better H1N1 specificity, although Ag-NP generally showed better antiviral activity and decreased cytotoxicity.

Keywords: Antiviral; Ag-NP; ZnO-NP; Adenovirus; HSV-2; Herpes; H1N1; Influenza

1. Introduction:

Throughout history, viral pandemics have had devastating consequences, leading to significant loss of life. The "Antonine Plague" in 165-180 CE, potentially caused by smallpox or measles, resulted in an estimated 5 million deaths [1,2]. The "Spanish Flu" of 1918-1919, caused by the H1N1 influenza A virus, caused an estimated 50-100 million deaths worldwide [3,4]. The ongoing HIV/AIDS, starting in 1981, has resulted in over 36 million deaths globally [4]. The COVID-19 pandemic caused by the SARS-CoV-2 virus has led to more than 3 million deaths worldwide [5]. The emergence of various virus strains poses a significant challenge in the prevention of viral infections. In response to the rapid changes in viral antigens, the extensive use of inactivated viral vaccines has been considered an effective approach [6,7]. However, the production of vaccines may not be sufficient to meet the increased demand during a viral pandemic [8]. While current treatments

can initially suppress viral infections, their long-term [9,10] effectiveness is often compromised by the emergence of drug-resistant strains [11]. Moreover, conventional antiviral agents, while effective, can have side effects or be toxic to normal healthy cells and essential microbial communities [12]. To address these challenges, researchers have explored alternative options such as silver nanoparticles [Ag-NP] and nano-composite as potential antiviral agents [13-15]. Ag-NPs have demonstrated promising antiviral properties against well-known viruses like influenza and human immunodeficiency virus (HIV), making them a potential avenue for combating viral infections while minimizing the risks of side effects and toxicity to healthy cells and beneficial microorganisms. The development of novel antiviral drugs, including (Ag-NP) and nano-composite, is crucial to effectively treat viral infections [9,10,13]. One of the prerequisites of sustainable development is the search for natural remedies, such as plant

*Corresponding author e-mail: amyoussef27@yahoo.com (Ahmed M. Youssef).

Receive Date: 31 July 2024, Revise Date: 31 August 2024, Accept Date: 10 September 2024

DOI: 10.21608/ejchem.2024.308604.10111

©2024 National Information and Documentation Center (NIDOC)

extracts and their derivatives, as alternatives to chemical therapies to lessen the issues caused by human-infecting viruses. Nanoparticles have garnered significant attention in recent years due to their distinctive properties and potential applications across various fields. Among these nanoparticles, silver and zinc oxide nanoparticles have demonstrated promise as effective antibacterial and antiviral agents, displaying potent inhibitory effects against a range of human viruses [16,17]. Furthermore, a critical area of research has evolved around the use of safe and sustainable synthesis methods for nanoparticle production [18].

The utilization of plant extracts as reducing and stabilizing agents in a process known as green synthesis has emerged as an eco-friendly and cost-effective approach to nanoparticle synthesis [19–21]. *Ficus carica*, commonly known as the Fig tree, is a readily available plant with medicinal properties that has been explored for its potential in nanoparticle synthesis [22]. Silver and zinc oxide nanoparticle production is effectively aided by a number of bioactive compounds present in *Ficus carica* leaf extract. These chemicals also inhibit the formation of metal ions [14,23,24]. Numerous studies have demonstrated successful green synthesis of silver nanoparticles using *Ficus carica* leaf extract. For instance, [25] reported the synthesis of silver nanoparticles utilizing *Ficus carica* leaf extract and evaluated their antiviral activity against human respiratory syncytial virus (HRSV). The results exhibited significant inhibition of HRSV replication, underscoring the potential of these nanoparticles as effective antiviral agents.

In addition to silver nanoparticles, zinc oxide nanoparticles synthesized using *Ficus carica* leaf extract have also displayed promising antiviral properties [26,27]. [28] were created zinc oxide nanoparticles from *Ficus carica* leaf extract and examined for their ability to combat the human immunodeficiency virus (HIV). By preventing HIV multiplication and the virus's entrance into host cells, these nanoparticles revealed strong antiviral effectiveness. The application of silver and zinc oxide nanoparticles, synthesized using *Ficus carica* leaf extract, as antiviral agents extends beyond their direct antiviral activity [2]. These nanoparticles are attractive prospects for a range of biomedical applications, such as drug delivery systems, diagnostic instruments, and therapeutic agents, since they also have other desirable qualities like durability, biocompatibility, and low toxicity [17]. Since, the green synthesis of silver and zinc oxide nanoparticles using *Ficus carica* leaf extract provides a sustainable and environmentally friendly approach. Our purpose was to use these nanoparticles as an antiviral agent against some human viruses and hold tremendous potential in

biomedical applications. Further research and development in this field are warranted to explore their comprehensive antiviral mechanisms and optimize their efficacy for practical implementation.

2. Materials and methods

2.1. Materials

Silver nitrate (AgNO_3), sodium hydroxide (pellet.99%) as the introduction material, and zinc acetate dihydrate (99% purity) were the primary components used in this study. They were all obtained from Sigma-Aldrich, USA Chemicals. *Ficus carica* fresh leaves were collected from faculty of Agriculture, Ain Shams University and were immediately transferred to the Laboratory for further processing.

2.2. Methods

2.2.1 Preparation of leaves extract

The plant leaves had to be washed twice, first with tap water and then with distilled water. Next, the leaves were laid out on a newspaper and let to dry in sunlight. Once dried, the leaves were finely ground to obtain a powdered form. Next, 10 grams of the fine leaf powder were combined with 100 milliliters of water and boiled for 15 minutes, while stirring constantly at 500 revolutions per minute using a magnetic stirrer. The resulting mixture was then left to cool for a period, filtered, and stored at a temperature of 4 degrees Celsius [29].

2.2.2. Nanoparticles synthesis

The zinc oxide and silver nanoparticles (ZnO-NP) and (Ag-NP), respectively were prepared according to method described by [29]. To prepare (ZnO-NP), 6 grams of zinc acetate were added to 60 milliliters of water. A solution of $\text{Zn}(\text{CH}_3\text{COO})_2 \cdot 2\text{H}_2\text{O}$ was added dropwise while boiling for 10 minutes at 50 degrees Celsius. The plant extract, 20 milliliters in volume, was also added. As a result, the color of the plant extract started to fade, and the pH of the solution was slightly acidic. To raise the pH, 2M NaOH solution was added until a pH of 11.5 was achieved. This led to a complete color change, and a cream-colored precipitate, indicating the formation of zinc hydroxide ($\text{Zn}(\text{OH})_2$), started to form. The precipitates were then washed, centrifuged at 7,000 rpm for 15 minutes, dried in an oven at 60 degrees Celsius, ground, and stored.

For the synthesis of Ag-NP, 10% (w/v) of leaf extract was mixed with a 6 mM solution of AgNO_3 in a ratio of 1:4, and constant stirring was applied. The appearance of a brown color indicated the reduction of Ag^+ to Ag^0 and the subsequent synthesis of Ag-NP. The mixture was then autoclaved for 5 minutes at 121 degrees Celsius and 15 psi. Afterward, the mixture was dispersed in distilled water, purified through centrifugation, dried

at 80 degrees Celsius, and stored at room temperature for future use.

2.3. Characterization of nanoparticles

2.3.1. UV-VIS characterization:

In this UV-Vis spectroscopy methodology, a spectral analysis was conducted using a V-730 UV-Visible Spectrophotometer with a high-resolution 1 nm spectral bandwidth, covering a spectral range from 700 nm to 200 nm, with data points acquired at 1 nm intervals. The measurements were carried out in a quartz cell, utilizing distilled water as the reference solvent. The instrument's linear dynamic range extended to over 3 absorbance units (AU) throughout the entire spectrum, ensuring accurate and precise data acquisition for the given wavelength range.

2.3.2. Transmission electron microscope (TEM)

The morphology of (Ag/Zn) NPs was examined using a transmission electron microscope (TEM), specifically the JEM-100CXII TEM instrument from Japan operating at 120 KV. The specimens were freshly prepared and the visualization was conducted by dropping the specimen solution.

2.3.4. X-ray diffraction (XRD)

The verification of Ag and Zn nanoparticles (NPs) was conducted using an X-ray diffraction (XRD) technique. The XRD measurements were performed on a Bruker diffractometer model called Bruker D 8 advance target. A $\text{Cu}\alpha$ radiation source with a secondary monochromator ($\lambda = 1.5405 \text{ \AA}$) was utilized, operating at 40 kV and 40 mA. The scanning rate for phase identification and line broadening profile analysis was set at 0.2 min^{-1} .

2.3.5. Antiviral and cytotoxicity of Ag and Zn nanoparticles

Nawah-Scientific in Egypt provided the three mentioned viruses and Madin-Darby canine kidney (MDCK) cells. The cells were grown in DMEM medium supplemented with 10% fetal bovine serum and 0.1% antibiotic/antimycotic solution, which was provided by Gibco BRL from Grand Island, NY, USA.

To evaluate antiviral activity and cytotoxicity, the Crystal violet method was used, following the previously reported cytopathic (CPE) inhibition effect by [30]. MDCK cells were cultured in a 96-well culture plate at a density of 2×10^4 cells/well one day prior to infection. The next day, the culture medium was removed, and the cells were washed with phosphate-buffered saline. The infectivity of the viruses was determined using the crystal violet method, which monitored CPE and allowed calculation of the percentage of cell viability. A diluted virus suspension of viruses containing CCID_{50} (1.0×10^6) of virus stock was added to the mammalian cells to induce desired CPEs two days after infection. For compound treatments, a medium containing the desired compound concentration was added to the cells. The antiviral activity of each test

sample was determined using 2-fold diluted concentrations ranging from 1000 $\mu\text{g/ml}$. Virus controls (virus-infected, non-drug-treated cells) and cell controls (non-infected, non-drug-treated cells) were included.

The culture plates were incubated at 37°C in 5% CO_2 for 72 hours, and the development of cytopathic effect was observed under light microscopy. The cell monolayers were then fixed, stained with a 0.03% crystal violet solution in 2% ethanol and 10% formalin, and the optical density of each well was quantified at 570/630 nm. The percentage of antiviral activity for each test compound was calculated according to [31] using the formula: antiviral activity = [(mean optical density of cell controls - mean optical density of virus controls) / (optical density of test - mean optical density of virus controls)] \times 100%. The IC_{50} (50% CPE inhibitory dose) was calculated based on these results. Prior to the assay, cytotoxicity was assessed by seeding cells at a density of 2×10^4 cells/well in a 96-well culture plate. The following day, the culture medium containing serially diluted samples was added to the cells and incubated for 72 hours. The cells were then washed with PBS, and the subsequent steps were carried out following the same procedure as described above for the antiviral activity assay. The IC_{50} (50% cytotoxic concentration) and IC_{50} values were determined using GraphPad PRISM software from Graph-Pad Software in San Diego, USA.

2.3.6. Statistical Analysis

(SPSS software version 25, Chicago, Illinois) a program for statistical analysis, Results was analyzed and summarized using the means \pm standard deviation. Significant P-values were defined as those less than 0.05 [32].

3.1. UV-VIS characterization of Ag-NP and ZnO - NPs

The UV-Vis spectroscopic analysis of Ag nanoparticles produced through green synthesis Figure (1a) revealed the presence of an absorbance peak at 445 nm [33]. This finding closely resembles the results reported in the study conducted by [34] providing strong evidence for the formation of silver nanoparticles (Ag-NP).

3.2. TEM characterization of Ag and Zn nanoparticles

The TEM analysis of (Ag-NP) and (ZnO-NP) showed that the nanoparticles with mean size ranges between 10.2 and 39.15 nm, and 22.86 and 44.47 nm respectively as shown in (Figure 2).

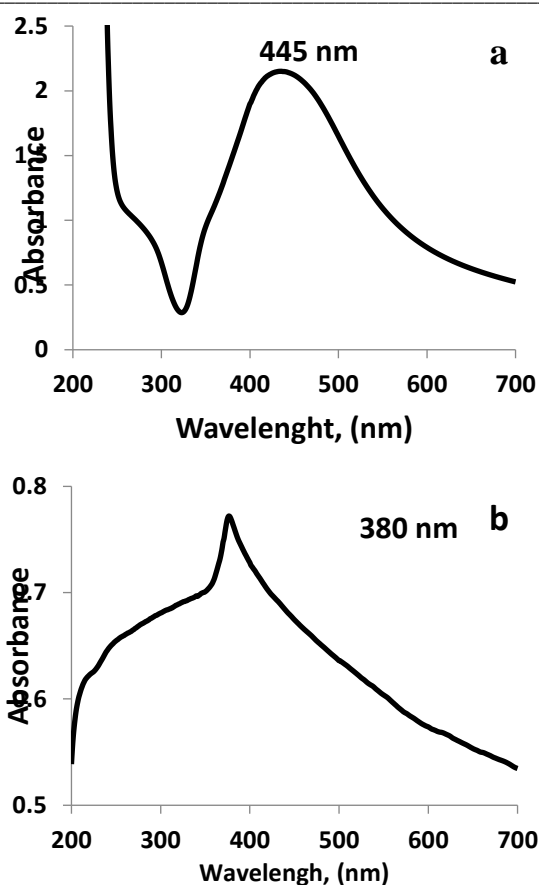


Figure 1. UV-Vis graph of a, (Ag-NP) and b, (Zn-NP) The UV-Vis absorbance spectrum of ZnO nanoparticles suspended in water is depicted in Figure 1(b). Within this spectrum, an absorption peak centered around 380 nm is observed, and this peak is recognized as a characteristic feature of hexagonal wurtzite ZnO, as reported by [35]. It's worth noting that this absorption peak exhibits a red shift of approximately 35 nm in comparison to bulk ZnO, as documented by [2,36]. This red shift can be attributed to the emergence of shallow energy levels within the band gap, a phenomenon likely induced by the presence of foreign atoms within the ZnO lattice. The shift of the absorption peak toward longer wavelengths signifies a reduction in the optical band gap, corresponding to the first bright exciting energy, as discussed by [37].

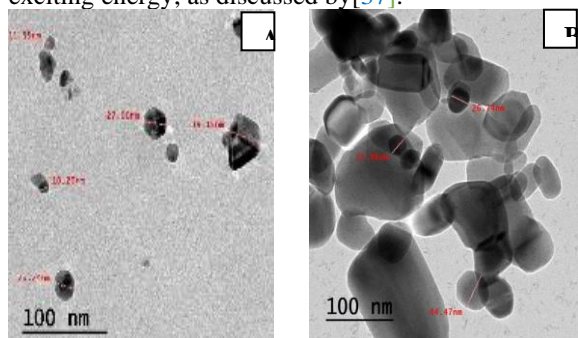


Figure 2: TEM image of (A) Ag-NP and (B) ZnO-NP

3.3. FT-IR of the green synthesized Ag and ZnO nanoparticles

The FTIR peak analysis of the green-synthesized Ag-NP revealed several unique peaks. As shown by the existence of peaks connected to O-H stretching vibrations, alcohols or phenols may be present as a result of the use of the green synthesis process [38,39]. It is possible that the stabilizing or reducing agents utilized in the green synthesis process are connected to the carbonyl groups present in aldehydes or ketones, as indicated by the observed peaks corresponding to C=O stretching vibrations [40]. Moreover, the peaks associated with C-H stretching vibrations indicate the presence of methyl groups or alkanes, which may be related to the stabilizers or capping agents utilized during the synthesis [41].

These metabolites prevent the nanoparticles from wrapping and aggregating [42]. The spectra show a strong similarity with only minor differences in peak positions, indicating a strong possibility that the sample contains residual plant extract that serves as a capping agent for the nanoparticles [43]. Consequently, it can be deduced that these biomolecules play a crucial role in both capping and effectively stabilizing the synthesized nanoparticles [38,44]. Green synthesized nanoparticles can additionally improve the therapeutic potential of plants and can be a source of new antiviral agents [45].

The FT-IR spectrum of ZnO nanoparticles Figure (3B) showed less peaks comparing with those related to the Ag nanoparticles. A strong absorption at 1820.45 cm^{-1} indicated the presence of C=O stretching vibrations, typically associated with carbonyl groups found in carboxylic acids or anhydrides. Another strong absorption at 1776.92 cm^{-1} suggested C=O stretching vibrations in carbonyl groups, commonly found in aldehydes, ketones, or esters. A medium absorption at 1427.29 cm^{-1} indicated C-H bending vibrations in alkane groups, while a medium absorption at 1166.40 cm^{-1} suggested the presence of C-O stretching vibrations in ethers or esters. Additionally, a medium absorption at 879.60 cm^{-1} suggested the bending vibrations of C-H bonds in aromatic compounds.

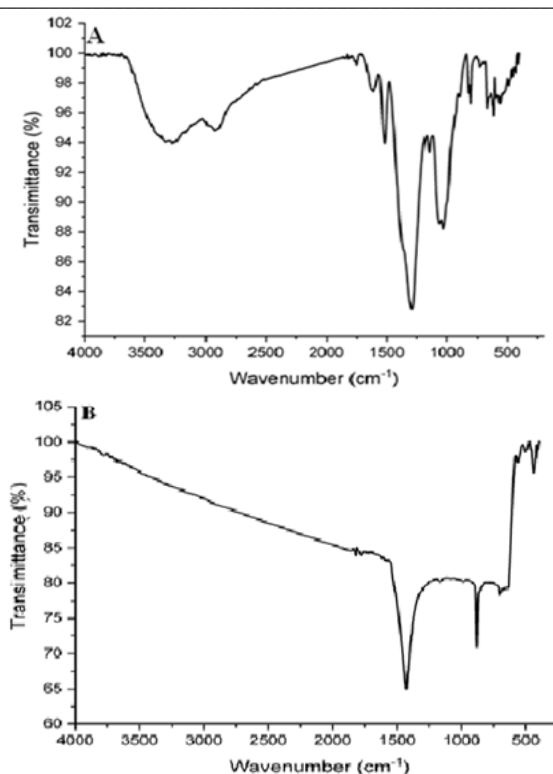


Figure 3: FT-IR spectra of nanoparticles synthesized by extract of *Ficus carica* A) Ag nanoparticles, B) ZnO nanoparticles

Several peaks displayed weak absorptions: 700.17 cm^{-1} indicated C-H bending vibrations in alkanes or alkyl groups, 561.49 cm^{-1} suggested the bending vibrations of C-H bonds in alkanes or alkyl groups, and 504.39 cm^{-1} indicated similar bending vibrations in alkane or alkyl groups. Overall, the FT-IR peak analysis of both the green synthesized (Ag-NP) and (ZnO-NP) provides valuable insights into their chemical composition and potential functional groups [2,46,47]. The synthesis of nanoparticles was successfully completed, and the surface properties of the nanoparticles' organic moieties are revealed by these observations. The green synthesis approach ensures the use of environmentally friendly methods and natural resources, making these nanoparticles promising candidates for biomedical applications [48,49].

3.4. Cytotoxicity and antiviral activity of ZnO /Ag-NP nanoparticles

Nanoparticles of zinc oxide (ZnO) and silver (Ag) have shown potential as medications for viral infection because of their distinct characteristics and possible modes of action [16,26]. These nanoparticles exhibit broad-spectrum antiviral activity against a range of viruses. The exact mechanisms by which Ag and ZnO nanoparticles exert their antiviral effects are still under investigation, but several potential mechanisms have been proposed. It has been reported also that NPs exhibit antiviral activity against numerous viruses, such as herpes simplex virus [50], hepatitis B[51] and H1N1[52].

3.4.1. Against Adenovirus

The results indicate that both ZnO/Ag nanoparticles exhibit antiviral activity against Adenovirus 40. ZnO nanoparticles have a CC_{50} of $119.430\text{ }\mu\text{g/ml}$, while Ag nanoparticles have a CC_{50} of $190.18\text{ }\mu\text{g/ml}$. This suggests that ZnO nanoparticles are relatively more cytotoxic to cells at higher concentrations compared to Ag nanoparticles. In terms of inhibitory concentration (IC_{50}) against Adenovirus 40, ZnO nanoparticles have an IC_{50} of $40.817\text{ }\mu\text{g/ml}$, while Ag nanoparticles have an IC_{50} of $40.41\text{ }\mu\text{g/ml}$. These values indicate that both types of nanoparticles require a similar concentration to effectively inhibit the virus. The selectivity index (SI) provides insights into the relative safety and selectivity of the nanoparticles towards the virus. ZnO nanoparticles have an SI of 2.9, while Ag nanoparticles have an SI of 4.7. This suggests that Ag nanoparticles exhibit a higher selectivity towards Adenovirus 40 compared to ZnO nanoparticles as revealed in (Figure 4 and Figure 5).

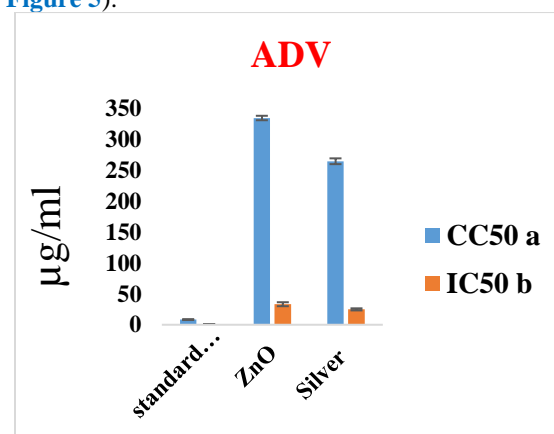


Figure 4: Cytotoxicity and antiviral activity of green synthesized nanoparticles of Ag and ZnO against adenovirus. CC_{50} was the concentration that showed viability of 50% of the host cells. IC_{50} was the concentration that inhibited 50% of ADV activity in direct anti-viral activity assay. Values are expressed as Mean \pm S.D *significantly different from the positive control group at $p < 0.05$.

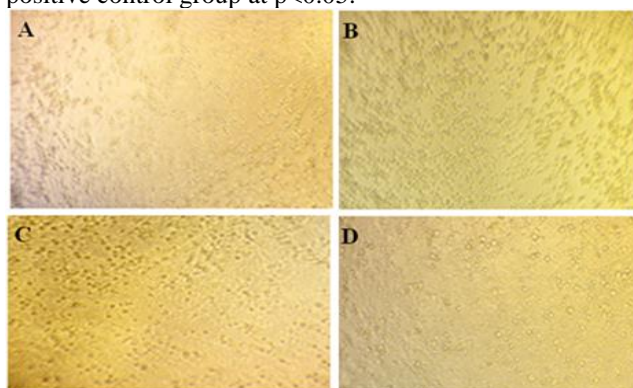


Figure 5: A) Cytotoxicity of Ag-NP, B) Viral control of Ag-NP, C) Cell control of Ag-NP and D) inhibitory effect of Ag-NP against adenovirus in MTT assay and the CPE method.

3.4.2. Against Human Herpes simplex virus type-2

The results designate that both Ag/ZnO nanoparticles exhibit antiviral activity against Human Herpes simplex virus type-2 (HSV-2). Ag nanoparticles have a CC_{50} of 187.076 $\mu\text{g/ml}$, while ZnO nanoparticles have a CC_{50} of 339.962 $\mu\text{g/ml}$. According to these data, ZnO nanoparticles appear to be less cytotoxic to cells than Ag nanoparticles with higher concentrations. In terms of inhibitory concentration (IC_{50}) against HSV-2, Ag nanoparticles have an IC_{50} of 22.585 $\mu\text{g/ml}$, while ZnO nanoparticles have an IC_{50} of 77.745 $\mu\text{g/ml}$.

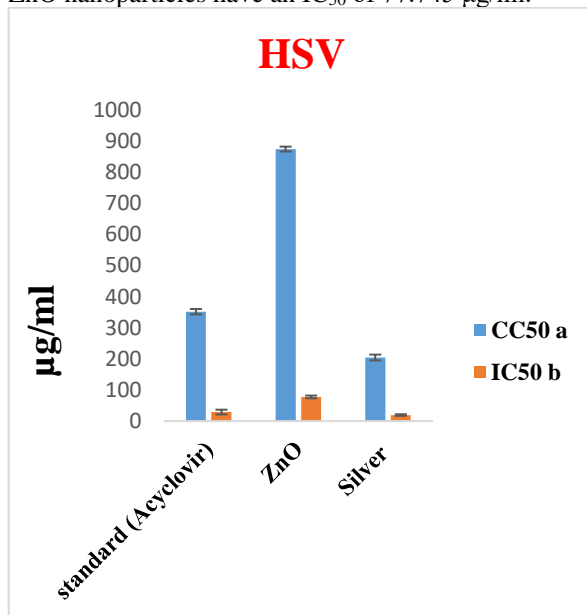


Figure 6: Cytotoxicity and antiviral activity of green synthesized nanoparticles of Ag and ZnO against Human Herpes simplex virus type-2. CC_{50} was the concentration that showed viability of 50% of the host cells. IC_{50} was the concentration that inhibited 50% of HSV activity in direct anti-viral activity assay. Values are expressed as Mean \pm S.D *significantly different from the positive control group at $p < 0.05$.

By comparing Ag and Zn nanoparticles, these values show that Ag nanoparticles need a lower concentration to effectively inhibit HSV-2. The selectivity index (SI) provides insights into the relative safety and selectivity of the nanoparticles towards the virus. Ag nanoparticles have an SI of 8.3, while Zn nanoparticles have an SI of 4.4. This suggests that Ag nanoparticles exhibit a higher selectivity towards HSV-2 compared to ZnO nanoparticles. These results suggest that Ag nanoparticles possess stronger antiviral activity against HSV-2 compared to ZnO nanoparticles. Ag nanoparticles exhibit a lower cytotoxicity to cells and a higher selectivity towards the virus. On the other hand, while ZnO nanoparticles also demonstrate antiviral activity, they exhibit a higher

cytotoxicity to cells and a slightly lower selectivity as shown in (Figure 6 and Figure 7)

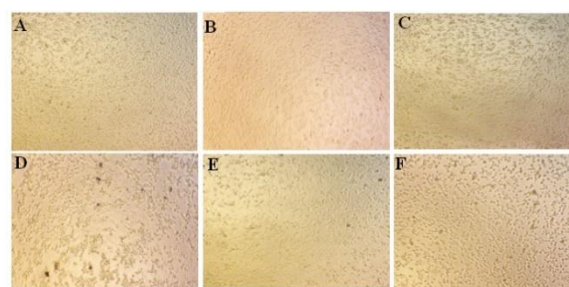


Figure 7: A) Cytotoxicity of 1000 of ZnO, B) Cell control of Ag-NP, C) Inhibitory effect of Ag-NP on Herpes, D) Cell Control for ZnO, E) Viral control for Ag-NP and F) Cytotoxicity of 1000 of Ag-NP against Herpes 2 virus in MTT assay and the CPE method.

3.4.3. Against H1N1 virus

The results indicate that both Ag/ZnO nanoparticles exhibit antiviral activity against H1N1 influenza virus. Ag nanoparticles have a CC_{50} of 58.23 $\mu\text{g/ml}$, while ZnO nanoparticles have a CC_{50} of 129.52 $\mu\text{g/ml}$. These values suggest that Ag nanoparticles are relatively more cytotoxic to cells at higher concentrations compared to ZnO nanoparticles. In terms of inhibitory concentration (IC_{50}) against H1N1, Ag nanoparticles have an IC_{50} of 23.03 $\mu\text{g/ml}$, while ZnO nanoparticles have an IC_{50} of 33.2 $\mu\text{g/ml}$. These values indicate that Ag nanoparticles require a lower concentration to effectively inhibit H1N1 compared to ZnO nanoparticles. The selectivity index (SI) indicates the relative safety and selectivity of the nanoparticles against the virus. Ag nanoparticles have a SI of 2.5, but ZnO nanoparticles have 3.9. This suggests that ZnO nanoparticles exhibit a higher selectivity towards H1N1 compared to Ag nanoparticles. These results suggest that ZnO nanoparticles possess relatively stronger antiviral activity against H1N1 compared to Ag nanoparticles. ZnO nanoparticles exhibit a lower cytotoxicity to cells and a higher selectivity towards the virus. On the other hand, while Ag nanoparticles also demonstrate antiviral activity, they exhibit a higher cytotoxicity to cells and a lower selectivity as demonstrated in (Figure 8 and Figure 9).

Ag nanoparticles with lower IC_{50} values and higher selectivity indices consistently show stronger antiviral activity against the three human viruses when compared to ZnO nanoparticles. They exhibit greater efficacy against Adenovirus 40 and Human Herpes simplex virus type-2 (HSV-2) compared to Zn nanoparticles. However, Ag nanoparticles also display higher cytotoxicity towards cells. Conversely, zinc nanoparticles show a moderate degree of antiviral activity and reduced cytotoxicity, despite having slightly higher IC_{50} values and lower

selectivity indices. These findings suggest that while Ag nanoparticles show stronger antiviral potential, Zn nanoparticles offer a balance between antiviral efficacy and reduced cytotoxicity. Further research is needed to explore their mechanisms of action and determine their optimal applications for combating these human viruses.

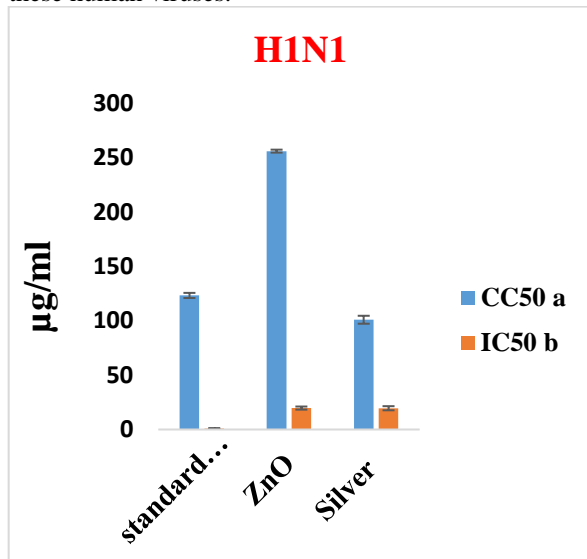


Figure 8: Cytotoxicity and antiviral activity of green synthesized nanoparticles of Ag and ZnO against H1N1 virus. CC₅₀ was the concentration that showed viability of 50% of the host cells. IC₅₀ was the concentration that inhibited 50% of H1N1 activity in direct anti-viral activity assay. Values are expressed as Mean \pm S.D. *significantly different from

The results indicate variations in the response of the three viruses, Adenovirus 40, Human herpes simplex virus type-2 (HSV-2), and H1N1 influenza virus, to the tested nanoparticles, Ag and ZnO. The antiviral activity of Ag nanoparticles was consistently higher than that of ZnO nanoparticles against all three viruses. Ag nanoparticles demonstrated increased selectivity indices (SI) and lower inhibitory concentrations (IC₅₀), indicating greater potency and selectivity against HSV-2 and Adenovirus 40. However, ZnO nanoparticles demonstrated a lower cytotoxicity towards cells. Interestingly, while Ag nanoparticles demonstrated higher antiviral efficacy against Adenovirus 40 and HSV-2, their potency against H1N1 influenza virus was relatively lower compared to ZnO nanoparticles. ZnO nanoparticles exhibited a moderate antiviral activity against H1N1 with a higher SI, indicating better selectivity, despite having slightly higher IC₅₀ values. the positive control group at $p < 0.05$

The viruses' susceptibility to specific routes of action or nanoparticle interactions may explain these responses. Every virus has distinct properties that can affect how it reacts to antiviral medications, such as its replication cycle, target host cells, and viral structure. Overall, the variations in response

highlight the complexity of virus-nanoparticle interactions and the importance of considering the specific characteristics of each virus when evaluating the potential of nanoparticles as antiviral agents. Further research is needed to gain a deeper understanding of these interactions and optimize the application of nanoparticles for effective antiviral strategies against different viral infections. The majority of the previous studies on (ZnO-NP) have focused on their ability to inhibit the growth of the different kinds of bacteria [46,53]. As a result, little is known about how (ZnO-NP) affects viruses in the literature that is currently in publication. Using alkaline zinc oxide to hydrolyze and neutralize virus particles is one possible antiviral method.

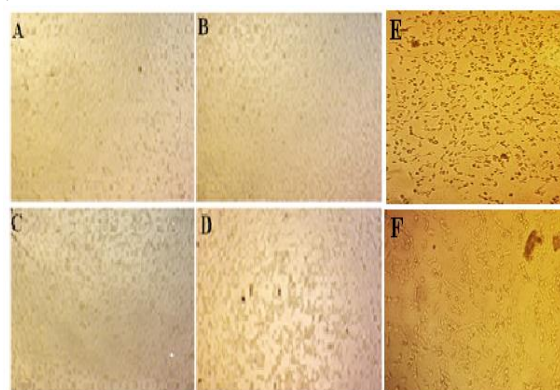


Figure 9: A) Cytotoxicity of ZnO-NP, B) Viral control of ZnO-NP, C) Cell control of ZnO-NP and D) inhibitory effect of ZnO-NP E) Inhibitory effect of Ag-NP on Virus and F) Cytotoxicity of Ag-NP against H1N1 virus in MTT assay and the CPE method.

In the case of the H1N1 influenza virus, both uncoated and PE-Gylated (ZnO-NP) were observed to impede the virus's replication within cells subsequent to infection. This inhibition might stem from the discharge of Zn²⁺ ions [2,26,54]. A comparable mechanism was also proposed by [55] for SARS-CoV-2. While analogous outcomes haven't been recorded for HSV or ADV, it is plausible to anticipate a similar process, which necessitates further investigation. The effectiveness of (ZnO-NP) against SARS-CoV-2 had been shown by tests conducted on VeroE6 cells, which revealed a significant reduction in the virus's protective envelope due to free radical activity producing oxidative stress [56,57]. Reactive oxygen species (ROS) generated by photocatalysis have the capacity to dismantle proteins, lipids, carbohydrates, and nucleic acids, ultimately leading to the deactivation of the virus [58] as revealed in (Figure 8).

Viral particles, such as glycoproteins found in the viral envelope, can directly interact with Ag and Zn nanoparticles, preventing their binding and entry into host cells [56,59]. This interaction, which disrupts the viral envelope or inhibits the virus's surface

proteins, may block the virus from reproducing and spreading [59,60]. Consequently, these nanoparticles can produce reactive oxygen species (ROS) like hydrogen peroxide, which can cause viruses to exhibit oxidative stress. Viral inactivation can occur in response to nucleic acids, proteins, and structures caused by elevated ROS levels [61].

Furthermore, Ag and ZnO nanoparticles may interfere with essential viral enzymes, such as proteases and polymerases, thereby disrupting viral replication and protein synthesis [15,33,62]. They can also modulate the host immune response by stimulating the production of antiviral cytokines and activating immune cells, enhancing the overall antiviral defense mechanisms [38]. Another proposed mechanism involves the interaction of Ag and ZnO nanoparticles with viral genetic material, such as RNA or DNA, hindering viral replication and transcription processes [15,63].

4. Conclusion

This study achieved the eco-friendly synthesis of silver (Ag-NP) and zinc oxide (ZnO-NP) nanoparticles through *Ficus carica* leaf extract. The investigation into antiviral and cytotoxic effects demonstrated both (Ag-NP) and (ZnO-NP) had antiviral properties, with (Ag-NP) showing superior efficacy and lower cytotoxicity against Adenovirus, HSV-2, and H1N1. These findings emphasize the potential of (Ag-NP) as potent antiviral agents and suggest their suitability for antiviral applications, offering promising avenues in the fight against viral infections. Further research and optimization could enhance their antiviral capabilities and selectivity, expanding their utility in antiviral therapies. In summary, the findings provide evidence that silver and zinc nanoparticles have efficient inhibitory activity on ADV, H1N1 and HSV viruses. Synthesized nanoparticles can also reduce the induced apoptosis toward cell lines cells according to TEM analysis. Further investigations are needed to clarify the mechanism of antiviral potential of the green synthesized Ag and Zn nanoparticles. Also, the application of Ag and ZnO nanoparticles as an effective drug against human viruses should be considered.

References

- [1] Stange N. Politics of Plague: Ancient Epidemics and Their Impact on Society. Claremont Coll Libr Undergrad Res Award. 2021;
- [2] Sofy AR, Sofy MR, Hmed AA, Dawoud RA, Alnaggar AEAM, Soliman AM, et al. Ameliorating the adverse effects of tomato mosaic tobamovirus infecting tomato plants in Egypt by boosting immunity in tomato plants using zinc oxide nanoparticles. *Molecules*. 2021;26(5):1–18.
- [3] Beštić-Bronza S. Spanish Flu 1918-1919 – Aspects of Demographic Implications. *Scr Medica (Banja Luka)*. 2020;51(2):110–9.
- [4] Silva S, Ayoub HH, Johnston C, Atun R, Abu-Raddad LJ. Estimated economic burden of genital herpes and HIV attributable to herpes simplex virus type 2 infections in 90 low- and middleincome countries: A modeling study. *PLoS Med* [Internet]. 2022;19(12):1–18. Available from: <http://dx.doi.org/10.1371/journal.pmed.1003938>
- [5] Adil MT, Rahman R, Whitelaw D, Jain V, Al-Ta'an O, Rashid F, et al. SARS-CoV-2 and the pandemic of COVID-19. *Postgrad Med J*. 2021;97(1144):110–6.
- [6] El-Gebaly A. a Predictive and Comparative Study Via Viral and Biochemical Measurements for Responders and Non-Responders Egyptian Hepatitis C Patients To Daclatasvir Plus Sofosbuvir Therapy. *Al-Azhar J Pharm Sci*. 2018;58(2):37–59.
- [7] Gupta S, Pellett S. Recent Developments in Vaccine Design: From Live Vaccines to Recombinant Toxin Vaccines. *Toxins (Basel)*. 2023;15(9).
- [8] Salari SA, Sadat, Sazvar Z. Designing a sustainable vaccine supply chain by considering demand substitution and value-added function during a pandemic outbreak. *Comput Ind Eng* [Internet]. 2024;187(October 2023):109826. Available from: <https://doi.org/10.1016/j.cie.2023.109826>
- [9] Badawy AA, Ghanem AF, Yassin MA, Youssef AM, Abdel Rehim MH. Utilization and characterization of cellulose nanocrystals decorated with silver and zinc oxide nanoparticles for removal of lead ion from wastewater. *Environ Nanotechnology, Monit Manag* [Internet]. 2021;16(June):100501. Available from: <https://doi.org/10.1016/j.enmm.2021.100501>
- [10] Jeevanandam J, Krishnan S, Hii YS, Pan S, Chan YS, Acquah C, et al. Synthesis approach-dependent antiviral properties of silver nanoparticles and nanocomposites. *J Nanostructure Chem* [Internet]. 2022;12(5):809–31. Available from: <https://doi.org/10.1007/s40097-021-00465-y>
- [11] Foka FET, Mufhandu HT. Current ARTs, Virologic Failure, and Implications for AIDS Management: A Systematic Review. *Viruses*. 2023;15(8).
- [12] Packialakshmi JS, Kang J, Jayakumar A, Park S, Chang Y, Kim JT. Insights into the antibacterial and antiviral mechanisms of metal oxide nanoparticles used in food packaging. *Food Packag Shelf Life* [Internet]. 2023;40(October):101213. Available from:

- <https://doi.org/10.1016/j.fpsl.2023.101213>
- [13] Sofy AR, Hmed AA, Abd El Haliem NF, Zein MAE, Elshaarawy RFM. Polyphosphonium-oligochitosans decorated with nanosilver as new prospective inhibitors for common human enteric viruses. *Carbohydr Polym* [Internet]. 2019;226(June):115261. Available from: <https://doi.org/10.1016/j.carbpol.2019.115261>
- [14] Saada NS, Abdel-Maksoud G, Abd El-Aziz MS, Youssef AM. Green synthesis of silver nanoparticles, characterization, and use for sustainable preservation of historical parchment against microbial biodegradation. *Biocatal Agric Biotechnol* [Internet]. 2021;32(February):101948. Available from: <https://doi.org/10.1016/j.bcab.2021.101948>
- [15] El-Gebaly AS, Sofy AR, Hmed AA, Youssef AM. Green synthesis, characterization and medicinal uses of silver nanoparticles (Ag-NPs), copper nanoparticles (Cu-NPs) and zinc oxide nanoparticles (ZnO-NPs) and their mechanism of action: A review. *Biocatal Agric Biotechnol* [Internet]. 2024;55(November 2023):103006. Available from: <https://doi.org/10.1016/j.bcab.2023.103006>
- [16] Mekky AE, Farrag AA, Hmed AA, Sofy AR. Antibacterial and antifungal activity of green-synthesized silver nanoparticles using spinacia oleracea leaves extract. *Egypt J Chem*. 2021;64(10):5781–92.
- [17] Asmat-Campos D, Rojas-Jaimes J, de Oca-Vásquez GM, Nazario-Naveda R, Delfín-Narciso D, Juárez-Cortijo L, et al. Biogenic production of silver, zinc oxide, and cuprous oxide nanoparticles, and their impregnation into textiles with antiviral activity against SARS-CoV-2. *Sci Rep* [Internet]. 2023;13(1):1–12. Available from: <https://doi.org/10.1038/s41598-023-36910-x>
- [18] Ali J, Bibi S, Jatoi WB, Tuzen M, Jakhrani MA, Feng X, et al. Green synthesized zinc oxide nanostructures and their applications in dye-sensitized solar cells and photocatalysis: A review. *Mater Today Commun* [Internet]. 2023;36(August):106840. Available from: <https://doi.org/10.1016/j.mtcomm.2023.106840>
- [19] El-Naggar ME, Gaballah S, Abdel-Maksoud G, El-Sayed HS, Youssef AM. Preparation of bactericidal zinc oxide nanoparticles loaded carboxymethyl cellulose/polyethylene glycol cryogel for gap filling of archaeological bones. *J Mater Res Technol* [Internet]. 2022;20:114–27. Available from: <https://doi.org/10.1016/j.jmrt.2022.07.013>
- [20] Wasilewska A, Klekotka U, Zambrzycka M, Zambrowski G, Święcicka I, Kalska-Szostko B. Physico-chemical properties and antimicrobial activity of silver nanoparticles fabricated by green synthesis. *Food Chem*. 2023;400(August 2022).
- [21] Kharey P, Goel M, Husain Z, Gupta R, Sharma D, M M, et al. Green synthesis of biocompatible superparamagnetic iron oxide-gold composite nanoparticles for magnetic resonance imaging, hyperthermia and photothermal therapeutic applications. *Mater Chem Phys* [Internet]. 2023;293(October 2022):126859. Available from: <https://doi.org/10.1016/j.matchemphys.2022.126859>
- [22] Rasool IF ul, Aziz A, Khalid W, Koraqi H, Siddiqui SA, AL-Farga A, et al. Industrial Application and Health Prospective of Fig (*Ficus carica*) By-Products. *Molecules*. 2023;28(3).
- [23] Arumugam J, Thambidurai S, Suresh S, Selvapandiyan M, Kandasamy M, Pugazhenthiran N, et al. Green synthesis of zinc oxide nanoparticles using *Ficus carica* leaf extract and their bactericidal and photocatalytic performance evaluation. *Chem Phys Lett* [Internet]. 2021;783(May):139040. Available from: <https://doi.org/10.1016/j.cplett.2021.139040>
- [24] Mouzahim M El, Eddarai EM, Eladaoui S, Guenbour A, Bellaouchou A, Zarrouk A, et al. Effect of Kaolin clay and *Ficus carica* mediated silver nanoparticles on chitosan food packaging film for fresh apple slice preservation. *Food Chem* [Internet]. 2023;410(January):135470. Available from: <https://doi.org/10.1016/j.foodchem.2023.135470>
- [25] Patil SP. *Ficus carica* assisted green synthesis of metal nanoparticles: A mini review. *Biotechnol Reports* [Internet]. 2020;28:e00569. Available from: <https://doi.org/10.1016/j.btre.2020.e00569>
- [26] Mekky AE, Farrag AA, Hmed AA, Sofy AR. Preparation of zinc oxide nanoparticles using *aspergillus niger* as antimicrobial and anticancer agents. *J Pure Appl Microbiol*. 2021;15(3):1547–66.
- [27] Moustafa H, Darwish NA, Youssef AM. Rational formulations of sustainable polyurethane/chitin/rosin composites reinforced with ZnO-doped-SiO₂ nanoparticles for green packaging applications. *Food Chem* [Internet]. 2022;371(May 2021):131193. Available from: <https://doi.org/10.1016/j.foodchem.2021.131193>
- [28] Rahman F, Majed Patwary MA, Bakar Siddique MA, Bashar MS, Haque MA, Akter B, et al. Green synthesis of zinc oxide nanoparticles using *Cocos nucifera* leaf extract: characterization, antimicrobial, antioxidant and photocatalytic activity. *R Soc Open Sci*. 2022;9(11).
- [29] Shamshad S, Rashid J, Ihsan-ul-haq, Iqbal N,

- Ullah Awan S. Synthesis of zinc oxide and silver nanoparticles using ficus palmata - Forssk leaf extracts and assessment of antibacterial activity. *Environ Eng Res*. 2020;26(6):200454–0.
- [30] Donalisio M, Nana HM, Ngono Ngane RA, Gatsing D, Tiabou Tchinda A, Rovito R, et al. In vitro anti-herpes simplex virus activity of crude extract of the roots of *nauclea latifolia smith* (rubiaceae). *BMC Complement Altern Med*. 2013;13.
- [31] Pauwels R, Balzarini J, Baba M, Snoeck R, Schols D, Herdewijn P, et al. Rapid and automated tetrazolium-based colorimetric assay for the detection of anti-HIV compounds. *J Virol Methods*. 1988;20(4):309–21.
- [32] Roos M, Stawarczyk B. Evaluation of bond strength of resin cements using different general-purpose statistical software packages for two-parameter Weibull statistics. *Dent Mater [Internet]*. 2012;28(7):e76–88. Available from: <http://dx.doi.org/10.1016/j.dental.2012.04.013>
- [33] Vinayagam R, Nagendran V, Goveas LC, Narasimhan MK, Varadavenkatesan T, Chandrasekar N, et al. Structural characterization of marine macroalgae derived silver nanoparticles and their colorimetric sensing of hydrogen peroxide. *Mater Chem Phys [Internet]*. 2024;313(November 2023):128787. Available from: <https://doi.org/10.1016/j.matchemphys.2023.128787>
- [34] Ali M, Kim B, Belfield KD, Norman D, Brennan M, Ali GS. Green synthesis and characterization of silver nanoparticles using *Artemisia absinthium* aqueous extract - A comprehensive study. *Mater Sci Eng C*. 2016;58:359–65.
- [35] Saleemi MA, Alallam B, Yong YK, Lim V. Synthesis of Zinc Oxide Nanoparticles with Bioflavonoid Rutin: Characterisation, Antioxidant and Antimicrobial Activities and In Vivo Cytotoxic Effects on *Artemia Nauplii*. *Antioxidants*. 2022;11(10).
- [36] Radičić R, Maletić D, Blažeka D, Car J, Krstulović N. Synthesis of Silver, Gold, and Platinum Doped Zinc Oxide Nanoparticles by Pulsed Laser Ablation in Water. *Nanomaterials*. 2022;12(19).
- [37] Sahu J, Kumar S, Vats VS, Alvi PA, Dalela B, Kumar S, et al. Lattice defects and oxygen vacancies formulated ferromagnetic, luminescence, structural properties and band-gap tuning in Nd³⁺ substituted ZnO nanoparticles. *J Lumin [Internet]*. 2022;243(September 2021):118673. Available from: <https://doi.org/10.1016/j.jlumin.2021.118673>
- [38] Youssef AM, El-Sayed HS, El-Nagar I, El-Sayed SM. Preparation and characterization of novel bionanocomposites based on garlic extract for preserving fresh Nile tilapia fish fillets. *RSC Adv*. 2021;11(37):22571–84.
- [39] Hassan Afandy H, Sabir DK, Aziz SB. Antibacterial Activity of the Green Synthesized Plasmonic Silver Nanoparticles with Crystalline Structure against Gram-Positive and Gram-Negative Bacteria. *Nanomaterials*. 2023;13(8).
- [40] Chaudhari RK, Shah PA, Shrivastav PS. Green synthesis of silver nanoparticles using *Adhatoda vasica* leaf extract and its application in photocatalytic degradation of dyes. *Discov Nano [Internet]*. 2023;18(1). Available from: <https://doi.org/10.1186/s11671-023-03914-5>
- [41] Vijayaraghavan K, Ashokkumar T. Plant-mediated biosynthesis of metallic nanoparticles: A review of literature, factors affecting synthesis, characterization techniques and applications. *J Environ Chem Eng [Internet]*. 2017;5(5):4866–83. Available from: <http://dx.doi.org/10.1016/j.jece.2017.09.026>
- [42] Sherin L, Sohail A, Amjad U e. S, Mustafa M, Jabeen R, Ul-Hamid A. Facile green synthesis of silver nanoparticles using *Terminalia bellerica* kernel extract for catalytic reduction of anthropogenic water pollutants. *Colloids Interface Sci Commun [Internet]*. 2020;37(September 2019):100276. Available from: <https://doi.org/10.1016/j.colcom.2020.100276>
- [43] John A, Shaji A, Velayudhannair K, M N, Krishnamoorthy G. Anti-bacterial and biocompatibility properties of green synthesized silver nanoparticles using *Parkia biglandulosa* (Fabales:Fabaceae) leaf extract. *Curr Res Green Sustain Chem [Internet]*. 2021;4(May):100112. Available from: <https://doi.org/10.1016/j.crgsc.2021.100112>
- [44] Habeeb Rahuman HB, Dhandapani R, Narayanan S, Palanivel V, Paramasivam R, Subbarayalu R, et al. Medicinal plants mediated the green synthesis of silver nanoparticles and their biomedical applications. *IET Nanobiotechnology*. 2022;16(4):115–44.
- [45] Jain N, Jain P, Rajput D, Patil UK. Green synthesized plant-based silver nanoparticles: therapeutic prospective for anticancer and antiviral activity. *Micro Nano Syst Lett [Internet]*. 2021;9(1). Available from: <https://doi.org/10.1186/s40486-021-00131-6>
- [46] Youssef A, El-Nagar I, El-Torky A, El-Hakim AEFA. Preparation and characterization of PMMA nanocomposites based on ZnO-NPs for antibacterial packaging applications. *Proc World Congr New Technol*. 2019;0:1–13.
- [47] Alprol AE, Mansour AT, El-Beltagi HS,

- Ashour M. Algal Extracts for Green Synthesis of Zinc Oxide Nanoparticles: Promising Approach for Algae Bioremediation. *Materials* (Basel). 2023;16(7):1–23.
- [48] Saada NS, Abdel-Maksoud G, Abd El-Aziz MS, Youssef AM. Green synthesis of silver nanoparticles, characterization, and use for sustainable preservation of historical parchment against microbial biodegradation. *Biocatal Agric Biotechnol* [Internet]. 2021;32(September 2020):101948. Available from: <https://doi.org/10.1016/j.bcab.2021.101948>
- [49] Samuel MS, Ravikumar M, John A, Selvarajan E, Patel H, Chander PS, et al. A Review on Green Synthesis of Nanoparticles and Their Diverse Biomedical and Environmental Applications. *Catalysts*. 2022;12(5).
- [50] Wang H, Xu X, Polla R La, Silva PJ, Ong QK, Stellacci F. Ligand concentration determines antiviral efficacy of silica multivalent nanoparticles. *J Colloid Interface Sci*. 2024;657(November 2023):327–33.
- [51] Kwon HJ, Kim HH, Yoon SY, Ryu YB, Chang JS, Cho KO, et al. In Vitro inhibitory activity of *Alpinia katsumadai* extracts against influenza virus infection and hemagglutination. *Virology*. 2010;7:1–9.
- [52] Dung TTN, Nam VN, Nhan TT, Ngoc TTB, Minh LQ, Nga BTT, et al. Silver nanoparticles as potential antiviral agents against African swine fever virus. *Mater Res Express*. 2019;6(12).
- [53] Sofy AR, Hmed AA, Alnaggar AEAM, Dawoud RA, Elshaarawy RFM, Sofy MR. Mitigating effects of Bean yellow mosaic virus infection in faba bean using new carboxymethyl chitosan-titania nanobiocomposites. *Int J Biol Macromol* [Internet]. 2020;163:1261–75. Available from: <https://doi.org/10.1016/j.ijbiomac.2020.07.066>
- [54] Ghaffari H, Tavakoli A, Moradi A, Tabarraei A, Bokharaei-Salim F, Zahmatkeshan M, et al. Inhibition of H1N1 influenza virus infection by zinc oxide nanoparticles: Another emerging application of nanomedicine. *J Biomed Sci*. 2019;26(1):1–10.
- [55] Wolfgruber S, Rieger J, Cardozo O, Punz B, Himly M, Stingl A, et al. Antiviral Activity of Zinc Oxide Nanoparticles against SARS-CoV-2. *Int J Mol Sci*. 2023;24(9).
- [56] Kubo AL, Rausalu K, Savest N, Žusinaite E, Vasiliev G, Viirsalu M, et al. Antibacterial and Antiviral Effects of Ag, Cu and Zn Metals, Respective Nanoparticles and Filter Materials Thereof against Coronavirus SARS-CoV-2 and Influenza A Virus. *Pharmaceutics*. 2022;14(12):1–19.
- [57] Sportelli MC, Izzi M, Loconsole D, Sallustio A, Picca RA, Felici R, et al. On the Efficacy of ZnO Nanostructures against SARS-CoV-2. *Int J Mol Sci*. 2022;23(6):1–12.
- [58] Idriss H, Habib M, Alakhras AI, El Khair HM. ZnO nanoparticles and their properties as surface coating materials against coronavirus: viewpoint. *J Optoelectron Biomed Mater*. 2022;14(2):53–61.
- [59] Jasim SA, Ahmed NS, Mousa AA, Hmed AA, Sofy AR. Correlation between both genetic polymorphism and serum level of toll-like receptor 4 with viral load and genotype of hepatitis C virus in Iraqi patients. *Gene Reports* [Internet]. 2021;24(July):101287. Available from: <https://doi.org/10.1016/j.genrep.2021.101287>
- [60] Sarkar J, Das S, Aich S, Bhattacharyya P, Acharya K. Antiviral potential of nanoparticles for the treatment of Coronavirus infections. *J Trace Elem Med Biol* [Internet]. 2022;72(March):126977. Available from: <https://doi.org/10.1016/j.jtemb.2022.126977>
- [61] Kaushik N, Mitra S, Baek EJ, Nguyen LN, Bhartiya P, Kim JH, et al. The inactivation and destruction of viruses by reactive oxygen species generated through physical and cold atmospheric plasma techniques: Current status and perspectives. *J Adv Res* [Internet]. 2023;43:59–71. Available from: <https://doi.org/10.1016/j.jare.2022.03.002>
- [62] Goharshadi EK, Goharshadi K, Moghayedi M. The use of nanotechnology in the fight against viruses: A critical review. *Coord Chem Rev* [Internet]. 2022;464:214559. Available from: <https://doi.org/10.1016/j.ccr.2022.214559>
- [63] Alavi M, Kamarasu P, McClements DJ, Moore MD. Metal and metal oxide-based antiviral nanoparticles: Properties, mechanisms of action, and applications. *Adv Colloid Interface Sci* [Internet]. 2022;306(June):102726. Available from: <https://doi.org/10.1016/j.cis.2022.102726>